Collective infrared excitation in rare-earth $Gd_xLa_{1-x}B_6$ hexaborides

E. S. Zhukova,[1,2] B. P. Gorshunov,[1,2,*] G. A. Komandin,[2] L. N. Alyabyeva,[1] A. V. Muratov,[3] Yu. A. Aleshchenko,[3] M. A. Anisimov,[2] N. Yu. Shitsevalova,[4] S. E. Polovets,[4] V. B. Filipov,[4] V. V. Voronov,[2] and N. E. Sluchanko[1,2]

[1]*Moscow Institute of Physics and Technology, 141700 Dolgoprudny, Moscow Region, Russia*

[2]*Prokhorov General Physics Institute of the Russian Academy of Sciences, 119991 Moscow, Russia*

[3]*Lebedev Physical Institute, Russian Academy of Sciences, 119991 Moscow, Russia*

[4]*Frantsevich Institute for Problems of Materials Science, National Academy of Sciences of Ukraine, 03680 Kiev, Ukraine*

(Received 10 November 2018; revised manuscript received 17 April 2019; published 5 September 2019)

Using Fourier-transform infrared spectroscopy and optical ellipsometry, room temperature spectra of complex conductivity of single crystals of hexaborides $Gd_xLa_{1-x}B_6$, $x(Gd) = 0, 0.01, 0.1, 0.78, 1$, are determined in the frequency range 30–35000 cm^{-1}. In all compounds, in addition to the Drude free-carrier spectral component, broad excitations are discovered with unusually large dielectric contributions $\Delta\varepsilon = 7\,000$–$15\,000$ and non-Lorentzian line shapes. It is suggested that the origin of the excitations is connected with the dynamic cooperative Jahn-Teller effect of B_6 clusters. Analysis of the spectra together with the results of dc and Hall resistivity measurements show that only 25–50% of the conduction band electrons are contributing to the free carrier ac conductivity, with the rest being involved in the formation of an overdamped excitation, thus providing a possible explanation, in terms of nonequilibrium (hot) electrons in these hexaborides, of both the remarkably low work function of thermoemission of $Gd_xLa_{1-x}B_6$ and the non-Fermi-liquid behavior in GdB_6 crystals.

DOI: 10.1103/PhysRevB.100.104302

I. INTRODUCTION

Rare earth (RE) borides RB_n (R is a metal ion, $n = 2, 4, 6, 12$, etc.) compose a large family of compounds that exhibit a broad variety of properties depending on the $n = [B]/[R]$ ratio and on the type of metallic atom hosted by the boron cage (in compounds with $n \geqslant 6$; for $n < 6$ the boron atoms form a *planar* network) [1]. Remarkable mechanical, chemical, and thermal characteristics determined by the boron framework of the systems make them promising for various technical applications in high performance electron sources, field- and thermal-induced emitters, sensors for high resolution detectors, electrical coatings for resistors, solid-state cryocooling elements, thermoelectric refrigerators, etc. [2–5]. In addition to promising practical applications, RE borides have an extremely rich set of intriguing physical properties. In this respect, especially attractive are borides with polyhedral-shaped boron cages ($n \geqslant 6$) with metal atoms residing within. It is the complicated interplay between large-amplitude rattling vibrations of these caged atoms, lattice dynamics, and electronic, magnetic and orbital subsystems that is expected to be at the origin of specific phenomena observed in RE borides and distinguishes them from other materials [6–11]. Corresponding collective interactions are usually characterized by relatively low energies, typically of the order of tens of meV or below. An effective experimental technique to study the origin of such interactions is provided by optical spectroscopy, that is able to deliver information on single-particle and collective excitations associated with charge, spin, orbital and phonon degrees of freedom, on microscopic parameters of charge carriers, and on the mixed-type phenomena involving different subsystems.

It is worth noting that while, indeed, Raman experiments are actively performed to study the optical response of borides, infrared (IR) spectroscopy, which is complementary to Raman spectroscopy, has not been used so often, especially in the most intriguing range of low energies (frequencies). The reason is the relatively high electrical conductivity of borides with $n \leqslant 12$ (except the narrow-gap semiconductors SmB_6 and YbB_{12}), that makes traditional IR Fourier-transform spectroscopy reflectivity measurements rather difficult due to the closeness of the reflection coefficient to 100%. In addition, the free charge carriers are very effective in screening dipole moments associated with possible IR-active excitations, making them hardly observable experimentally. As a result, IR experiments are rather scarce and relate mainly to the investigations of high-energy interband transitions.

To fill the gap in the studies of low-energy electrodynamic properties of RE borides, we performed in [12] measurements of the broadband IR spectrum of LuB_{12}, a dodecaboride with a lutetium ion that is nonmagnetic excluding additional complications due to magnetoelastic effects and strong electron correlations. Especially careful measurements below 10 000 cm^{-1}, where the reflection coefficient of dodecaborides gets strongly enhanced, allowed us to discover a broad non-Lorentzian line shaped IR excitation with unusually large dielectric contribution ($\Delta\varepsilon \approx 8\,000$). We have associated its origin with cooperative dynamics of Jahn-Teller (JT) active B_{12} complexes that produce quasilocal vibrations (rattling modes) of caged lutetium ions. The conclusion was also supported by the results of quantum chemical calculations and geometry optimizations for a charged $[B_{12}]^{2-}$ cluster [13] which revealed JT splitting of the triply degenerate highest

*bpgorshunov@gmail.com

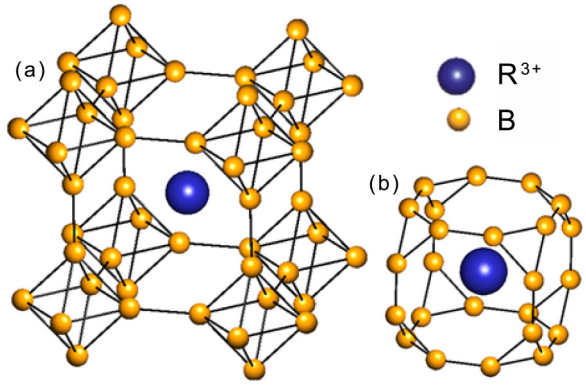

FIG. 1. (a) Crystal structure of RB_6. (b) Fedorov B_{24} polyhedra centered by R^{3+} ion.

occupied molecular orbital and symmetry lowering. Moreover, very recently it was found that the cooperative dynamic JT instability of the boron sublattice serves as the reason for the formation of dynamic charge stripes in the cage-cluster LuB_{12} compound [14]. The aim of the present work is to apply a similar approach for the search of low-energy excitations and thus for the study of the nature of the ground states of two representatives of RE metallic hexaborides, LaB_6 and GdB_6, and their solid solutions $Gd_xLa_{1-x}B_6$.

RB_6 compounds crystallize in a bcc structure of CsCl type with $Pm3m$-O_1^h symmetry where a loosely bound RE atom is located at the Cs site and an octahedral B_6 complex occupies the Cl position [Fig. 1(a)]. As a result, there are two subsystems in the crystal structure. One of them is the rigid boron covalent network and another is loosely bound R^{3+} ions embedded in cavities [B_{24} cubo-octahedra; see Fig. 1(b)] of the boron cage [15,16]. For this reason vibrations of the heavy ions in RB_6 show flat and low-energy dispersion branches [Einstein oscillators with the temperatures $\Theta_E(LaB_6) \approx 140$–$150$ K and $\Theta_E(GdB_6) \approx 91$ K] [17–19], and the amplitude of these rattling modes in GdB_6 is among the largest in the whole RB_6 family [17].

Special interest in higher borides LaB_6 and GdB_6 is caused by two reasons. First, both have an extremely low work function of thermoemission [$\varphi(LaB_6) \approx 2.66$ eV, $\varphi(GdB_6) \approx 2.51$ eV] [20–24], making one of them (LaB_6) the most commonly used material for thermionic cathodes in various electron-beam devices. In particular, the most effective electron-beam sources of high brightness used for various purposes, such as electron microscopy and microfabrication of super-large-scale integrated circuits, are built based on LaB_6 crystals [22–31]. It should be noted that the physical origin of the LaB_6 high thermoemission efficiency is not clear at present, and this stimulates corresponding active studies (see, e.g., [32]). Second, these two compounds attract active research interest due to their exotic fundamental physical properties. Indeed, LaB_6 is a nonmagnetic reference compound in the RB_6 family which possesses diverse and unusual electronic and magnetic properties, including homogeneous intermediate valence with a topological Kondo insulating ground state in SmB_6 [33,34], heavy fermionic behavior with unusual multipole magnetic ordering in CeB_6 [35,36], a complex magnetic ground state in PrB_6–HoB_6 antiferromagnets [37–40], and itinerant ferromagnetic behavior in EuB_6 [41].

Depending on the RE or transition-metal ion, these compounds can be narrow-gap semiconductors (SmB_6, YbB_6 [42,43]), semimetals (EuB_6 [41,44,45]), antiferromagnetic metals (PrB_6–HoB_6 [37,40,46,47]) and superconductors (YB_6 [48]). Among the antiferromagnetic hexaborides, GdB_6 is an S-state system (for Gd^{3+}, $L = 0$, $S = 7/2$), but demonstrates a non-Fermi-liquid behavior of the resistivity $\rho \sim T$ [47] and two successive antiferromagnetic transitions which are accompanied by simultaneous structural distortions [39,47,49]. Linear behavior of resistivity was found earlier in high-temperature superconducting cuprates [50–54], pnictides [55,56], and organic superconductors [57,58] as well as in many heavy fermion metals and superconductors [59,60] including those located in the vicinity of the quantum critical point (QCP) [61]. Various mechanisms have been proposed to explain the effect, including quantum critical theories [61] and more exotic approaches, but its nature is still the subject of active debate. As was shown recently by the analysis of experimental results obtained for $Sr_3Ru_2O_7$ in the vicinity of QCP [62], the linear dependence of resistivity can be characterized by the same carrier scattering rate in different types of conductors; a single description can thus be offered in terms of the quantum diffusion transport of charge carriers [59].

The described rich variety of properties of RE borides clearly indicates the existence of collective effects whose optical fingerprints in the form of collective excitations are typically expected to exist at infrared and far-infrared frequencies. Anomalous peaks have been observed below 200 cm^{-1} in the Raman spectra of RB_6 (R = Ca, Ce, Pr, Gd, Dy, and Yb) [6,7] and attributed to local rattling vibrations of the R ions in a shallow and unharmonic potential created by the boron cage. In [8–11] optical and infrared conductivity spectra of a series of hexaborides were measured in the energy range from 1 meV to 40 eV. The observed excitations were analyzed and assigned to interband transitions. It was noted in [9] that the optical conductivity spectra between ≈400 cm^{-1} (≈50 meV) and ≈8 000 cm^{-1} (≈1 eV) obtained by Kramers-Kronig analysis for a number of hexaborides (including LaB_6) could not be fitted with the simple Drude conductivity model. The effect was attributed to the electron-phonon and electron-electron scattering and modeled by introducing a frequency-dependent scattering rate (and effective mass) of conduction electrons, giving a strong indication of the presence of collective interactions in hexaborides.

To shed more light on the nature of such interactions, in the present study we measured the room temperature broadband infrared reflectivity spectra of $Gd_xLa_{1-x}B_6$ single crystals with a series of gadolinium concentrations: $x(Gd) = 0$ (LaB_6), 0.01, 0.1, 0.78, 1 (GdB_6). Exceptionally high quality of single-crystalline samples and extension of the measurement frequency interval down to as low as 30 cm^{-1} (corresponding to the energy of ≈4 meV) made it possible to discover overdamped infrared excitations in these compounds characterized by non-Lorentzian line shapes. Comparative analysis of these collective excitations with that observed recently in a broadband conductivity spectra of LuB_{12} allows us to associate their origin with the dynamic cooperative

Jahn-Teller effect of B_6 clusters. Analyzing the temperature dependence of the Drude conductivity spectra of free carriers and of the overdamped excitations and their evolution with x(Gd), we conclude that the $Gd_xLa_{1-x}B_6$ hexaborides are *nonequilibrium metals*. In these metals only 25–50% of electrons in the conduction band contribute to the free carrier conductivity. The rest of the carriers are involved in the formation of many-body complexes that in turn are responsible for strong changes in the $5d$-$2p$ hybridization and hence for the modulation of the conduction band.

II. EXPERIMENTAL DETAILS

High quality $Gd_xLa_{1-x}B_6$ single crystals were grown by vertical crucible-free inductive zone melting in argon gas atmosphere on the setup described in detail in [63]. The sample quality was characterized carefully by x-ray diffraction, microprobe and optical spectral analysis, and magnetization and dc transport measurements. For optical measurements samples $\approx 5 \times 5\ \mathrm{mm}^2$ in area were used with surfaces polished with diamond powder, planar within $\pm 1\ \mu$m. To avoid structural distortions on the surface, all samples were etched in dilute nitric acid. The reflection coefficient $R(\nu)$ spectra were measured using a Vertex 80V Fourier-transform spectrometer in the range of frequencies 30–8000 cm^{-1}. Gold films deposited on glass substrates were used as reference mirrors. Using a J. A. Woollam V-VASE ellipsometer, spectra of optical parameters [optical conductivity $\sigma(\nu)$ and real part of dielectric permittivity $\varepsilon'(\nu)$] of the samples were directly determined in the interval 3700–35000 cm^{-1} with a frequency resolution of 50 cm^{-1}. Measurements with a radiation spot diameter of 2 mm were provided with angles of incidence of 65°, 70°, and 75°. From the ellipsometry data, reflection coefficients were calculated using standard Fresnel expressions and merged with the measured IR spectra. The data from [11] were used to extend the spectra up to $\approx$400 000 cm^{-1}. The obtained broadband reflection coefficient spectra were analyzed as described below. dc conductivities σ_{dc} and Hall resistivity of the same samples were measured using a standard five-probe method.

III. RESULTS AND DISCUSSION

Figure 2 shows the reflection coefficient spectra of LaB_6 and GdB_6 that represent the two limiting compositions of the $Gd_xLa_{1-x}B_6$ series. Features above 30 000 cm^{-1} (data from [11]) are related to interband transitions and will not be discussed here. First of all, we note that although the overall $R(\nu)$ spectra look typically metal-like (there is a characteristic plasma edge at $\approx$17 000 cm^{-1} and the reflectivity approaches 100% at frequencies below $\approx$1000 cm^{-1}) they cannot be reproduced by the expression for the complex conductivity given by the Drude model:

$$\sigma^*_{\mathrm{Drude}}(\nu) = \frac{\sigma_{\mathrm{dc}}^{\mathrm{Drude}}}{1 - i\nu/\gamma^{\mathrm{Drude}}}, \tag{1}$$

where $\sigma_{\mathrm{dc}}^{\mathrm{Drude}}$ is the dc conductivity and γ^{Drude} is the charge-carrier scattering rate. This is demonstrated by the dashed lines in Fig. 2, which show the best possible fit to experimental spectra using expression (1) alone. A similar mismatch between experiment and Drude fit was observed for all our $Gd_xLa_{1-x}B_6$ samples, with the deviations deceasing with the increase in x(Gd).

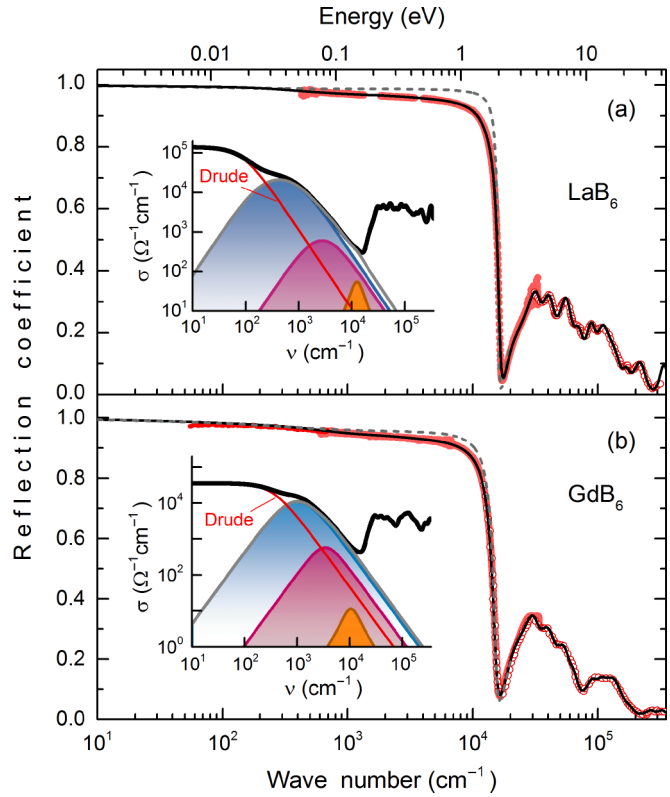

FIG. 2. Room temperature reflection coefficient spectra of the LaB_6 (a) and GdB_6 (b) crystals. Dots show experimental data obtained using a Fourier-transform spectrometer and an ellipsometer, as described in the text. Open circles correspond to high-frequency reflectivity data from [64]. Solid lines show the results of fitting the spectra using the Drude term, Eq. (1), for the free charge carrier response and Lorentzians, Eq. (2), responsible for absorption resonances. Dashed lines show best fits of the spectra that can be obtained using the Drude conductivity term alone with $\sigma_{\mathrm{dc}} = 139\,715\ \Omega^{-1}\mathrm{cm}^{-1}$, $\gamma^{\mathrm{Drude}} = 330\ \mathrm{cm}^{-1}$ for LaB_6 and $\sigma_{\mathrm{dc}} = 35\,460\ \Omega^{-1}\mathrm{cm}^{-1}$, $\gamma^{\mathrm{Drude}} = 1050\ \mathrm{cm}^{-1}$ for GdB_6. Insets present separately infrared contributions to the conductivity spectra (shown by black dots) from free carriers (Drude) and Lorentzians.

To reveal the phenomena responsible for the detected effects, we derived the spectra of optical conductivity by processing the reflection coefficient spectra with Kramers-Kronig analysis. For high frequencies ν^{-4} extrapolations were used. Towards low frequencies the spectra were extrapolated with the Hagen-Rubens expression $R(\nu) = 1 - \sqrt{4\nu/\sigma_{\mathrm{dc}}}$. In addition, we performed spectral analysis of the reflectivity spectra by fitting them with expression (1) together with the minimal set (two to four, dependent on the composition; see insets in Fig. 2) of Lorentzians needed to reproduce the measured $R(\nu)$ spectra:

$$\sigma^*(\nu) = \frac{0.5 f \nu}{\nu\gamma + i\left(\nu_0^2 - \nu^2\right)}. \tag{2}$$

In Eq. (2), $\Delta\varepsilon$ is the dielectric contribution, ν_0 is the resonance frequency, $f = \Delta\varepsilon\nu_0^2$ is the oscillator strength, and γ

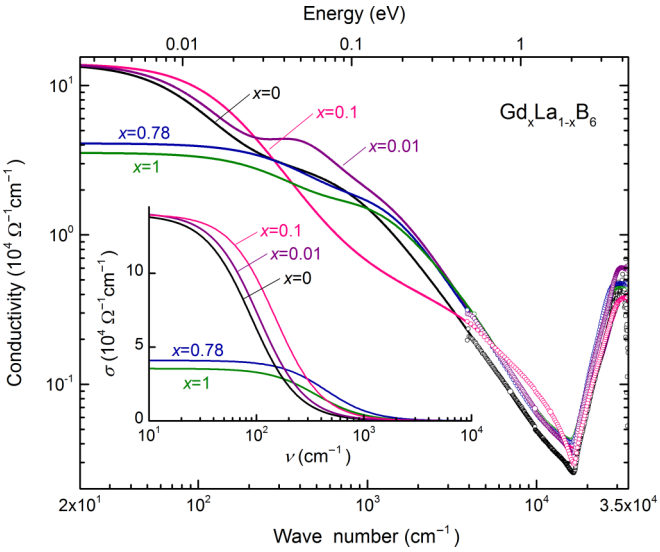

FIG. 3. Room temperature spectra of the real part of conductivity of $Gd_xLa_{1-x}B_6$ crystals. The spectra are obtained by least-square fitting of the reflection coefficient spectra using the Drude conductivity term, Eq. (1), and Lorentzian terms, Eq. (2). The inset shows just the Drude conductivity spectra. Dots correspond to data *directly* measured by the ellipsometer.

is the damping constant. Both methods provided basically the same results that are presented in Fig. 3 in the form of optical conductivity $\sigma(\nu)$ spectra of all studied $Gd_xLa_{1-x}B_6$ crystals. The spectra are shown for frequencies above 30 cm^{-1}—where they were essentially independent of various low-frequency extrapolations during Kramers-Kronig analysis—and up to 35 000 cm^{-1}, the highest frequency in our experiment. Lines in this figure present the results of fitting the broadband reflectivity spectra obtained by merging the reflectivity (a) directly measured with the Fourier-transform spectrometer (30–8 000 cm^{-1}) and (b) calculated using the conductivity (dots in the figure) and permittivity results obtained by ellipsometry, as mentioned above.

In the main panel of Fig. 3 one can clearly distinguish Drude-like conductivity increase towards low frequencies below 200–300 cm^{-1} together with several absorption bands at $\nu \geqslant 200$ cm^{-1}. The Drude free-carrier contributions to the conductivity spectra are shown separately in the inset. The dependence of the charge carrier scattering rate and of the dc conductivity on the gadolinium content is presented in Fig. 4(a) and in Table I. Smooth and significant (by ~5 times) growth of the scattering rate and corresponding decrease of the dc conductivity are observed when the concentration of Gd increases towards $x(\mathrm{Gd}) = 1$ in GdB_6. The absorption bands have rather unusual characteristics. First, these bands are clearly seen in the reflectivity and conductivity spectra and are not completely screened by the charge carriers in the samples. Second, Lorentzian terms [Eq. (2)] used to reproduce their spectral shape are characterized by relatively large values of oscillator strengths $f \sim (1\text{–}2) \times 10^9$ cm^{-2}, dielectric contributions $\Delta\varepsilon \sim 7\,000\text{–}15\,000$ and damping constants $\gamma/\nu_0 \sim 1\text{–}3$. This means that the corresponding absorption mechanisms cannot be connected with regular phonons or interband transitions.

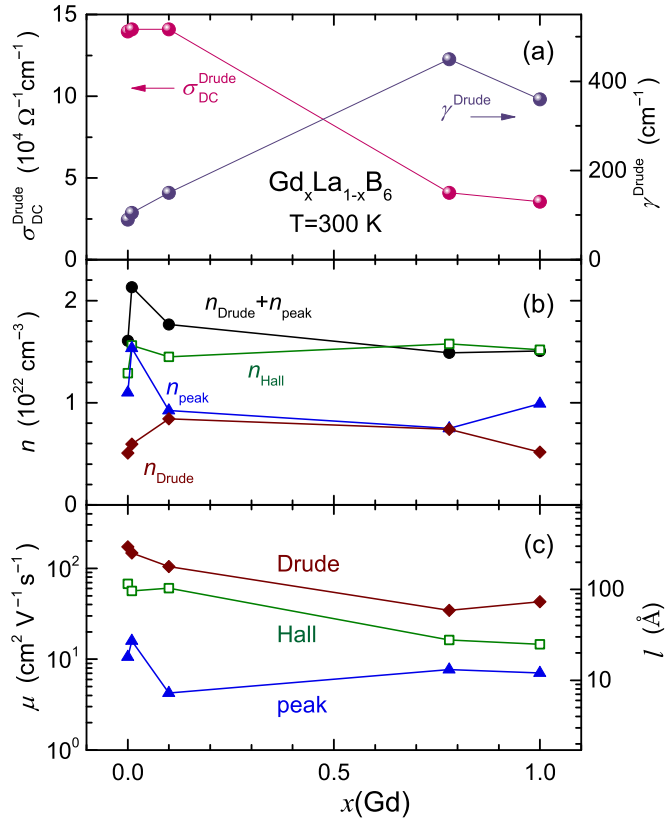

FIG. 4. (a) Dependencies on the gadolinium concentration of charge carrier parameters that are responsible for the Drude conductivity in $Gd_xLa_{1-x}B_6$: dc conductivity σ_{dc}^{Drude} and scattering rate γ^{Drude}. Panel (b) shows the same dependencies for free charge carrier concentration n_{Drude}, concentration n_{peak} of electrons responsible for the formation of collective absorption peaks, combined concentration $n_{Drude} + n_{peak}$, and the concentration n_{Hall} of carriers obtained from Hall effect measurements. (c) Dependence on x(Gd) of charge carrier mobility and mean-free path obtained at room temperature from optical experiments and from Hall effect measurements. See also Table I. ("Drude" denotes carriers responsible for the Drude contribution in the spectra, see inset in Fig. 3; "peak" denotes electrons participating in the formation of collective excitations).

We believe that the obtained overall conductivity spectra of all samples, in addition to the Drude components connected with free carriers, contain intense collective excitations with pronouncedly non-Lorentzian line shapes. This effect was formally reproduced here by fitting the spectra with a sum of several terms given by Eq. (2). We show these excitations in Fig. 5(a) in the form of absorption peaks obtained by subtraction of the Drude components from the overall conductivity spectra. [We note that there are signs of weak bands around 10^4 cm^{-1} that could be associated with interband transitions. Their oscillator strengths, however, are one or two orders of magnitude smaller than those of the components that mainly determine the intensities of the peaks (see insets in Fig. 2)].

We assume that the origin of the discovered overdamped excitations is connected with the Jahn-Teller instability of the B_6 complexes composed of natural boron (a mixture of ^{10}B and ^{11}B isotopes) which leads to emergence of a cooperative dynamic JT effect. We suggest that this kind of nonadiabatic mechanism launching both the cooperative

TABLE I. Parameters of the Drude conductivity, Eq. (1), and the peak terms [composed by Lorentzians, Eq. (2); see text] used to describe the room temperature reflectivity spectra of $Gd_xLa_{1-x}B_6$ crystals. Examples of spectra for LaB_6 and GdB_6 are presented in Fig. 2. Drude term: σ_{dc}^{Drude} is the measured dc conductivity; γ^{Drude} is the charge carrier scattering rate; ν_{pl}^{Drude} is the charge carrier plasma frequency; n_{Drude} is the charge carrier concentration. Peak term: f_{peak} and $\Delta\varepsilon_{peak}$ are the oscillator strength [sum of the oscillator strengths of four Lorentzian terms, Eq. (2), that compose the collective peak; see Fig. 5(a)] and the dielectric contribution (sum of the dielectric contributions of four Lorentzian terms that compose the collective peak), respectively; γ_{peak} is the damping [half-height width of collective peak composed by four Lorentzian terms, Eq. (2)]; ν_{peak} is the position of the collective peak maximum; γ_{peak}/ν_{peak} is the relative damping.

x(Gd)	σ_{dc}^{Drude} ($\Omega^{-1}cm^{-1}$)	γ^{Drude} (cm^{-1})	$(\nu_{pl}^{Drude})^2$ ($10^9 cm^{-2}$)	f_{peak} ($10^9 cm^{-2}$)	$\Delta\varepsilon_{peak}$	ν_{peak} (cm^{-1})	γ_{peak} (cm^{-1})	γ_{peak}/ν_{peak}
0	139715	90	0.75	1.64	7726	430	1470	3.42
0.01	141000	105	0.89	2.29	7500	410	980	2.3
0.1	141000	150	1.27	1.38	14850	1110	3665	3.3
0.78	40980	450	1.1	1.1	15500	1100	2024	1.85
1	35460	360	0.77	1.48	15000	965	2207	2.3

overdamped modes and electronic instability could provide the most natural interpretation of the anomalies observed in the $\sigma(\nu)$ spectra. It is seen from Figs. 5(a) and 5(b) and Table I that, with the growth of Gd content from $x(Gd) = 0$ to $x(Gd) = 1$, the collective absorption peak is blueshifted by about 2.5 times in frequency and its dielectric contribution is nearly tripled. At the same time, the oscillator strength shows only slight tendency to decrease.

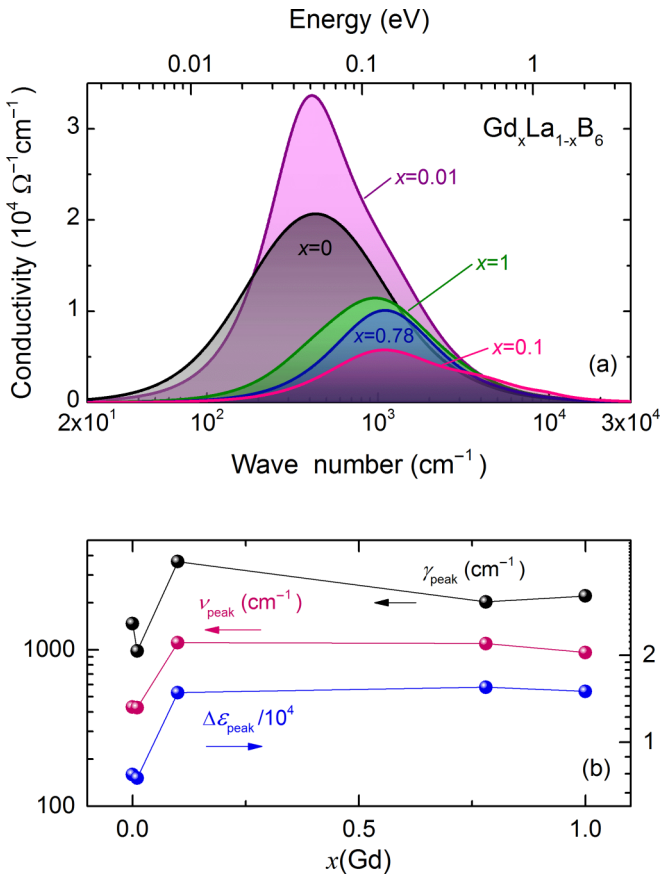

FIG. 5. (a) Collective absorption peaks observed at room temperature in $Gd_xLa_{1-x}B_6$ crystals and modeled by a sum of Lorentzian terms, Eq. (2), as discussed in the text. (b) Dependence on the gadolinium concentration of the absorption peak parameters: dielectric contribution $\Delta\varepsilon_{peak}$, peak frequency position ν_{peak}, and damping constant γ_{peak}. See also Table I.

Taking the value of the electronic effective mass $m^* = 0.6m_0$ [46] (m_0 is free electron mass), and using the relations for charge carrier plasma frequency $\nu_{pl} = [n_{Drude}e^2/(\pi m^*)]^{1/2}$ (n is the concentration of free electrons, e their charge) and oscillator strength of the Lorentzians $f = \Delta\varepsilon\nu_0^2 = ne^2(\pi m^*)^{-1}$, we can estimate the concentration n_{Drude} of free carriers participating in the Drude conductivity and the concentration n_{peak} of the charge carriers involved in the formation of the overdamped excitations. The results are presented in Fig. 4(b), together with the total concentration $n_{Drude} + n_{peak}$ that reveals only slight decrease when x(Gd) changes from 0 to 1. According to the estimates, for all studied compositions 50–75% of electrons in the conduction band are involved in the formation of the collective excitations, with the highest fraction of more than ≈75% detected in LaB_6. Only the remaining 25–50% of the carriers directly participate in the conduction process.

It is worth noting that the total concentration $n_{Drude} + n_{peak}$ found from optical measurements practically coincides with the concentration $n_{Hall} = (R_H e)^{-1}$ obtained from Hall effect measurements on the same samples (R_H is the Hall coefficient). This leads us to conclude that during the charge transport experiments significant contribution to the detected Hall signal is made, along with the Drude charge carriers, also by the nonequilibrium (hot) electrons participating in collective vibrations. We note here that these hot electrons should not be regarded as completely localized, and their origin may be explained as follows. (i) Because of the JT instability, two or more (degenerate or pseudodegenerate) electronic states of each boron cluster B_6 become mixed under JT vibrations via a nonadiabatic coupling [65]. (ii) In the hexaboride matrix, the collective JT effect on the lattice of these B_6 complexes is at the origin of both the collective dynamics of boron clusters and the large amplitude vibrations of the RE ions. (iii) These rattling modes of R^{3+} ions necessarily initiate strong changes in the $5d$-$2p$ hybridization of R and boron electronic states. (iv) Since the states in the conduction band are composed of the antibonding orbitals of the B_6 molecule and the $5d$ orbitals of the La (Gd) atoms [66–68], the variation of the $5d$-$2p$ hybridization will lead to the modulation of conduction

band width and consequent generation of the nonequilibrium (hot) charge carriers.

Our finding in $Gd_xLa_{1-x}B_6$ of the two types of conduction electrons ("regular" and hot) is confirmed by an estimate of the total carrier concentrations from the Hall effect data, $n_{\mathrm{Hall}} \approx (1.4\text{–}1.6) \times 10^{22}$ cm^{-3}. This value coincides well with that obtained from the reflectivity measurements, $n_{\mathrm{Drude}} + n_{\mathrm{peak}} = (1.5\text{–}2.2) \times 10^{22}$ cm^{-3}, with the electronic concentration obtained assuming one electron in the conduction band per unit cell and with the previously obtained results of transport measurements [46,69]. Furthermore, we can calculate mobility $\mu = e\tau/m^* = e(2\pi m^* \gamma^{\mathrm{Drude}})^{-1}$ and mean-free path $l = v_F\tau$ of the carriers responsible for the Drude transport [here $v_F \approx 6 \times 10^7$ cm/s is the Fermi velocity detected in [70,71] and $\tau = (2\pi\gamma^{\mathrm{Drude}})^{-1}$ is the relaxation time]. Figure 4(c) demonstrates that the increase of gadolinium content leads to significant decrease of the mobility and mean-free path. Such behavior should be attributed to the carrier scattering on magnetic Gd ions and on their rattling vibrations, whose amplitude is significantly larger compared to that of La ions [17–19]. It is worth noting that the mobility and mean-free path values determined from the Hall effect measurements are lower than those of the free charge carriers (Drude) but higher than the values found for the hot electrons involved in the collective mode (peak). This is consistent with the proposed idea of the presence in the studied compounds of two types of electrons. In the Hall experiments, the mobility and mean-free path of *all* charge carriers are determined. Their concentration is given by $n_{\mathrm{Drude}} + n_{\mathrm{peak}}$ and includes the free (Drude) and the nonequilibrium (peak) electrons with relatively large and small mobilities and mean free paths, respectively.

The cooperative JT dynamics of boron complexes B_6 that is suggested here to explain the origin of the discovered collective excitation in RB_6 compounds leads to two effects. First, the cooperative high-frequency JT boron vibrations provoke the rattling modes of heavy RE ions. These modes are quasilocal low-frequency vibrations whose equivalent Einstein temperature $\Theta_E = 90\text{–}150$ K (dependent on the R ion) is too small to be detected in optical spectra. However, these modes are reliably detected in studies of heat capacity and in inelastic neutron scattering measurements [17–19]. Second, since the RE ions are loosely bound in the rigid boron RB_6 cage, the Einstein oscillators are characterized by very large vibration amplitude that leads to strong variation of the $5d$-$2p$ hybridization of the R and boron ions. As a result, modulation of the conduction band occurs that produces "hot charge carriers" which are strongly scattered on the quasilocal mode.

In our opinion, the discovered large fraction of conduction electrons involved in the formation of collective excitation should be considered in terms of the nonequilibrium charge carriers, thus providing a possible explanation of the remarkably low work function of thermoemission in $Gd_xLa_{1-x}B_6$ hexaborides. It is worth noting also that although the work function of thermoemission in GdB_6 is slightly lower than in LaB_6 [20–24] the concentration of hot electrons (n_{peak}) in the latter is significantly higher [see Fig. 4(b)]. This explains the highest brightness of the cathodes on the basis of lanthanum hexaboride. Moreover, these nonequilibrium and strongly scattered electrons in the RE hexaborides should be certainly taken into account when explaining the emergence of the non-Fermi-liquid regime of the charge transport in GdB_6 with the linear temperature dependence of resistivity [47,49,69].

IV. CONCLUSIONS

Room temperature spectra of infrared conductivity of single-crystalline $Gd_xLa_{1-x}B_6$ [x(Gd) = 0, 0.01, 0.1, 0.78, 1] rare-earth hexaborides are determined in the frequency range 30–35 000 cm^{-1}. It is demonstrated that the spectra contain two main contributions. The first is related to the response of free charge carriers and is described basing on the Drude conductivity model. In addition, an overdamped excitations with unusually large dielectric contributions $\Delta\varepsilon = 7\,000\text{–}15\,000$ and oscillator strengths $f \sim (1\text{–}2) \times 10^9$ cm^{-2} are discovered whose origin is associated with the dynamic cooperative Jahn-Teller effect of B_6 clusters. The dependencies of parameters of both spectral components on gadolinium content x(Gd) are determined and analyzed. It is shown that only 25–50% of the conduction band electrons are contributing to the free carrier conductivity, with the rest being involved in the formation of the collective excitations. The latter observation of the nonequilibrium (hot) electrons with nonadiabatic coupling to the lattice vibrations is supposed to be at the origin of the remarkably low work function of thermoemission of $Gd_xLa_{1-x}B_6$ crystals and may be responsible for emergence of the non-Fermi-liquid regime of the charge transport in GdB_6.

ACKNOWLEDGMENTS

The research was supported by the Russian Science Foundation under Grant No. 17–12–01426 and by the Ministry of Education and Science of the Russian Federation (Program 5 top 100). The authors acknowledge the Shared Facility Center at the P. N. Lebedev Physical Institute of RAS for using their equipment.

[1] T. Mori, in *Rare Earth Borides, Carbides and Nitrides*, edited by D. A. Atwood (John Wiley & Sons, Chichester, 2012), p. 263.
[2] G. Balakrishnan, M. R. Lees, D. McK. Paul, J. Mag. Mag. Mat. **272-276**, 601 (2004).
[3] L. Bao, J. Zhang, S. Zhou, N. Zhang, and H. Xu, Chin. Phys. Lett. **28**, 088101 (2011).
[4] V. Petrosyan, V. Vardanyan, V. Kuzanyan, M. Konovalov, V. Gurin, and A. Kuzanyan, Solid State Sci. **14**, 1653 (2012).
[5] J. Q. Xu, T. Mori, Y. Bando, D. Golberg, D. Berthebaud, and A. Prytuliak, Mater. Sci. Eng. B **177**, 117 (2012).
[6] N. Ogita, S. Nagai, N. Okamoto, M. Udagawa, F. Iga, M. Sera, J. Akimitsu, and S. Kunii, Physica B **329-333**, 661 (2003).

[7] N. Ogita, T. Hasegawa, M. Udagawa, F. Iga, and S. Kunii, J. Phys.: Conf. Ser. **176**, 012032 (2009).

[8] S. Kimura, T. Nanba, M. Tomikawa, S. Kunii, and T. Kasuya, Phys. Rev. B **46**, 12196 (1992).

[9] S.-i. Kimura, T. Nanba, S. Kunii, and T. Kasuya, Phys. Rev. B **50**, 1406 (1994).

[10] S. Kimura, H. Harima, T. Nanba, S. Kunii, and T. Kasuya, J. Phys. Soc. Jpn. **60**, 745 (1991).

[11] S. Kimura, T. Nanba, S. Kunii, and T. Kasuya, J. Phys. Soc. Jpn. **59**, 3388 (1990).

[12] B. P. Gorshunov, E. S. Zhukova, G. A. Komandin, V. I. Torgashev, A. V. Muratov, Yu. A. Aleshchenko, S. V. Demishev, N. Yu. Shitsevalova, V. B. Filipov, and N. E. Sluchanko, JETP Lett. **107**, 100 (2018).

[13] N. Sluchanko, A. Bogach, N. Bolotina, V. Glushkov, S. Demishev, A. Dudka, V. Krasnorussky, O. Khrykina, K. Krasikov, V. Mironov, V. B. Filipov, and N. Shitsevalova, Phys. Rev. B **97**, 035150 (2018).

[14] N. B. Bolotina, A. P. Dudka, O. N. Khrykina, V. N. Krasnorussky, N. Yu. Shitsevalova, V. B. Filipov, and N. E. Sluchanko, J. Phys.: Condens. Matter. **30**, 265402 (2018).

[15] D. Mandrus, B. C. Sales, and R. Jin, Phys. Rev. B **64**, 012302 (2001).

[16] M. A. Anisimov, V. V. Glushkov, A. V. Bogach, S. V. Demishev, N. A. Samarin, S. Yu. Gavrilkin, K. V. Mitsen, N. Yu. Shitsevalova, A. V. Levchenko, V. B. Filipov, S. Gabáni, K. Flachbart, and N. E. Sluchanko, J. Exp. Theor. Phys. **116**, 760 (2013).

[17] K. Iwasa, R. Igarashi, K. Saito, C. Laulhé, T. Orihara, S. Kunii, K. Kuwahara, H. Nakao, Y. Murakami, F. Iga, M. Sera, S. Tsutsui, H. Uchiyama, and A. Q. R. Baron, Phys. Rev. B **84**, 214308 (2011).

[18] M. Korsukova, in *Proceedings of the 11th International Symposium on Boron, Borides, and Related Compounds, 22-26 August 1993, Tsukuba (Japan)*, edited by R. Uno and I. Higashi (Japanese Journal of Applied Physics, Tokyo, 1994), p.15.

[19] Y. Takahashi, K. Ohshima, F. P. Okamura, S. Otani, and T. Tanaka, J. Phys. Soc. Jpn. **68**, 2304 (1999).

[20] M. Bakr, K. Yoshida, S. Ueda, M. Takasaki, R. Kinjo, Y. W. Choi, H. Zen, T. Sonobe, T. Kii, K. Masuda, and H. Ohgaki, in *Proceedings of the 1st International Particle Accelerator Conference (IPAC'10), 23-28 May 2010, Kyoto (Japan)*, edited by S. Kurokawa and K. Oide (JACoW, Geneva, Switzerland, 2010), p. 1782.

[21] J. M. Lafferty, J. Appl. Phys. **22**, 299 (1951).

[22] L. W. Swanson and T. Dickinson, Appl. Phys. Lett. **28**, 578 (1976).

[23] C. Oshima, E. Bannai, T. Tanaka, and S. Kawai, J. Appl. Phys. **48**, 3925 (1977).

[24] M. Aono, T. Tanaka, E. Bannai, and S. Kawai, Appl. Phys. Lett. **31**, 323 (1977).

[25] L. W. Swanson, M. Gesley, and D. R. McNeely, NASA Technical Memo NSG-3054, 1977.

[26] B. Goldstein and D. J. Szostak, Surf. Sci. **74**, 461 (1978).

[27] A. Berrada, J. P. Mercurio, J. Etourneau, F. Alexandre, and J. B. Theeten, Surf. Sci. **72**, 177 (1978).

[28] A. N. Broers, J. Appl. Phys. **38**, 1991 (1967); **38**, 3040 (1967); J. Phys. E **2**, 273 (1969); Rev. Sci. Instrum. **40**, 1040 (1969); J. Vac. Sci. Technol. **10**, 979 (1973).

[29] S. F. Vogel, Rev. Sci. Instrum. **41**, 585 (1970).

[30] J. D. Verhoeven and E. D. Gibson, J. Phys. E **9**, 65 (1976).

[31] R. Shimizu, T. Shinike, S. Ichimura, S. Kawai, and T. Tanaka, J. Vacuum Sci. Technol. **15**, 922 (1978).

[32] M. Trenary, Sci. Tech. Adv. Mat. **13**, 023002 (2012).

[33] M. Dzero, K. Sun, V. Galitski, and P. Coleman, Phys. Rev. Lett. **104**, 106408 (2010).

[34] D. J. Kim, J. Xia, and Z. Fisk, Nat. Mater. **13**, 466 (2014).

[35] A. S. Cameron, G. Friemel, and D. S. Inosov, Rep. Prog. Phys. **79**, 066502 (2016).

[36] M. Sera, K. Kunimori, T. Matsumura, A. Kondo, H. Tanida, H. Tou, and F. Iga, Phys. Rev. B **97**, 184417 (2018).

[37] C. M. McCarthy, C. W. Tompson, R. J. Graves, H. W. White, Z. Fisk, and H. R. Ott, Solid State Commun. **36**, 861 (1980).

[38] C. M. McCarthy and C. W. Tompson, J. Phys. Chem. Sol. **41**, 1319 (1980).

[39] M. Amara, S. E. Luca, R.-M. Galéra, F. Givord, C. Detlefs, and S. Kunii, Phys. Rev. B **72**, 064447 (2005).

[40] K. Segawa, A. Tomita, K. Iwashita, M. Kasaya, T. Suzuki, and S. Kunii, J. Magn. Magn. Mater. **104-107**, 1233 (1992).

[41] S. Süllow, I. Prasad, M. C. Aronson, S. Bogdanovich, J. L. Sarrao, and Z. Fisk, Phys. Rev. B **62**, 11626 (2000).

[42] N. E. Sluchanko, V. V. Glushkov, B. P. Gorshunov, S. V. Demishev, M. V. Kondrin, A. A. Pronin, A. A. Volkov, A. K. Savchenko, G. Grüner, Y. Bruynseraede, V. V. Moshchalkov, and S. Kunii, Phys. Rev. B **61**, 9906 (2000).

[43] Y. Zhou, D.-J. Kim, Priscila Ferrari Silveira Rosa, Q. Wu, J. Guo, S. Zhang, Z. Wang, D. Kang, W. Yi, Y. Li, X. Li, J. Liu, P. Duan, M. Zi, X. Wei, Z. Jiang, Y. Huang, Y.-f. Yang, Z. Fisk, L. Sun, and Z. Zhao, Phys. Rev. B **92**, 241118(R) (2015).

[44] S. Massidda, A. Continenza, T. M. de Pascale, and R. Monnier, Z. Phys. B: Condens. Mat. **102**, 83 (1997).

[45] M. C. Aronson, J. L. Sarrao, Z. Fisk, M. Whitton, and B. L. Brandt, Phys. Rev. B **59**, 4720 (1999).

[46] Y. Onuki, A. Umezawa, W. K. Kwok, G. W. Crabtree, M. Nishihara, T. Yamazaki, T. Omi, and T. Komatsubara, Phys. Rev. B **40**, 11195 (1989).

[47] S. Kunii, K. Takeuchi, I. Oguro, K. Sogiyama, A. Ohya, M. Yamada, Y. Koyoshi, M. Date, and T. Kasuya, J. Magn. Magn. Mater. **52**, 275 (1985).

[48] N. Sluchanko, V. Glushkov, S. Demishev, A. Azarevich, M. Anisimov, A. Bogach, V. Voronov, S. Gavrilkin, K. Mitsen, A. Kuznetsov, I. Sannikov, N. Shitsevalova, V. Filipov, M. Kondrin, S. Gabáni, and K. Flachbart, Phys. Rev. B **96**, 144501 (2017).

[49] M. Anisimov, V. Glushkov, A. Bogach, S. Demishev, N. Samarin, A. Samarin, N. Shitsevalova, A. Levchenko, V. Filipov, S. Gabáni, K. Flachbart, and N. Sluchanko, Acta Phys. Pol. A **131**, 973 (2017).

[50] M. Gurvitch and A. T. Fiory, Phys. Rev. Lett. **59**, 1337 (1987).

[51] K. Takenaka, K. Mizuhashi, H. Takagi, and S. Uchida, Phys. Rev. B **50**, 6534 (1994).

[52] Y. Ando, K. Segawa, S. Komiya, and A. N. Lavrov, Phys. Rev. Lett. **88**, 137005 (2002).

[53] A. W. Tyler, Y. Ando, F. F. Balakirev, A. Passner, G. S. Boebinger, A. J. Schofield, A. P. Mackenzie, and O. Laborde, Phys. Rev. B **57**, R728(R) (1998).

[54] T. Watanabe, T. Fujii, and A. Matsuda, Phys. Rev. Lett. **79**, 2113 (1997).

[55] H. Takahashi, T. Okada, Y. Imai, K. Kitagawa, K. Matsubayashi, Y. Uwatoko, and A. Maeda, Phys. Rev. B **86**, 144525 (2012).
[56] M. Abdel-Hafiez, J. Ge, A. N. Vasiliev, D. A. Chareev, J. Van de Vondel, V. V. Moshchalkov, and A. V. Silhanek, Phys. Rev. B **88**, 174512 (2013).
[57] N. Doiron-Leyraud, S. René de Cotret, A. Sedeki, C. Bourbonnais, L. Taillefer, P. Auban-Senzier, D. Jérome, and K. Bechgaard, Eur. Phys. J. B **78**, 23 (2010).
[58] J. S. Brooks, Rep. Prog. Phys. **71**, 126501 (2008).
[59] T. Hu, Y. Liu, H. Xiao, G. Mu, and Y.-f. Yang, Sci. Rep. **7**, 9469 (2017).
[60] R. Daou, C. Bergemann, and S. R. Julian, Phys. Rev. Lett. **96**, 026401 (2006).
[61] G. R. Stewart, Rev. Mod. Phys. **78**, 743 (2006); **73**, 797 (2001).
[62] J. A. N. Bruin, H. Sakai, R. S. Perry, and A. P. Mackenzie, Science **339**, 804 (2013).
[63] G. Friemel, Y. Li, A. V. Dukhnenko, N. Yu. Shitsevalova, N. E. Sluchanko, A. Ivanov, V. B. Filipov, B. Keimer, and D. S. Inosov, Nat. Commun. **3**, 830 (2012).
[64] H. Okamura, S. Kimura, H. Shinozaki, T. Nanba, F. Iga, N. Shimizu, and T. Takabatake, Phys. Rev. B **58**, R7496(R) (1998).
[65] I. B. Bersuker, *The Jahn-Teller Effect* (Cambridge University Press, Cambridge, 2015), p. 616.
[66] K. Takegahara and T. Kasuya, Solid State Commun. **53**, 21 (1985).
[67] P. F. Walch, D. E. Ellis, and F. M. Mueller, Phys. Rev. B **15**, 1859 (1977).
[68] Y. Kubo and S. Asano, Phys. Rev. B **39**, 8822 (1989).
[69] M. A. Anisimov, A. V. Bogach, V. V. Glushkov, S. V. Demishev, N. A. Samarin, V. B. Filipov, N. Yu. Shitsevalova, and N. E. Sluchanko, arXiv:1006.0124.
[70] Yu. S. Ponosov and S. V. Strel'tsov, JETP Lett. **97**, 447 (2013).
[71] Y. Ishizawa, T. Tanaka, E. Bannai, and S. Kawai, J. Phys. Soc. Jpn. **42**, 112 (1977).